31st Annual International Conference of the IEEE EMBS
Minneapolis, Minnesota, USA, September 2-6, 2009

# Optimization of Doppler velocity echocardiographic measurements using an automatic contour detection method

E. Gaillard, L. Kadem, P. Pibarot and L.-G. Durand

*Abstract*— **Intra- and inter-observer variability in Doppler velocity echocardiographic measurements (DVEM) is a significant issue. Indeed, imprecisions of DVEM can lead to diagnostic errors, particularly in the quantification of the severity of heart valve dysfunction. To minimize the variability and rapidity of DVEM, we have developed an automatic method of Doppler velocity wave contour detection, based on active contour models. To validate our new method, results obtained with this method were compared to those obtained manually by an experienced echocardiographer on Doppler echocardiographic images of left ventricular outflow tract and transvalvular flow velocity signals recorded in 30 patients, 15 with aortic stenosis and 15 with mitral stenosis. We focused on three essential variables that are measured routinely by Doppler echocardiography in the clinical setting: the maximum velocity, the mean velocity and the velocity-time integral. Comparison between the two methods has shown a very good agreement (linear correlation coefficient $R^2 = 0.99$ between the automatically and the manually extracted variables). Moreover, the computation time was really short, about 5s. This new method applied to DVEM could, therefore, provide a useful tool to eliminate the intra- and inter-observer variabilities associated with DVEM and thereby to improve the diagnosis of cardiovascular disease. This automatic method could also allow the echocardiographer to realize these measurements within a much shorter period of time compared to standard manual tracing method. From a practical point of view, the model developed can be easily implanted in a standard echocardiographic system.**

## I. Introduction

Doppler velocity echocardiographic measurements (DVEM) remain highly dependent on the person who performs them [1-5]. From data found in the literature, Margulescu et al. [5] have shown an important intra- and inter-observer variability of DVEM. For example, Kupfahl et al. [4], in 2004, have shown that the assessment variability of the aortic stenosis severity by Doppler echocardiography is very high with both transthoracic and transoesophageal echocardiography (28% to 41% and 25% to 43%, respectively). These imprecisions of DVEM can lead to errors in the assessment of the severity of the heart valve disease. Accurate assessment of disease severity is crucial for selection of the appropriate treatment. It is, therefore, important to minimize intra- and inter-observer variability when performing Doppler echocardiographic measurements. Moreover, the Doppler echocardiographic measurements are generally performed by manual tracing (using a track ball) on at least 3 cardiac beats in patients with sinus rhythm and on 5 cardiac cycles in patients with atrial fibrillation. These measurements are therefore time consuming.

In view of these observations, we developed an automatic method of Doppler velocity contour detection based on active contour models. Active contour models (or snakes) were first introduced by Kass et al. [6] in 1988, and have quickly gained popularity in different domains. They have proven to be useful in medical image analysis [7-9] and for tracking moving objects in video [10-12]. The concept of snakes is based on curve detection through an optimization process. This optimization makes use of models of curve contrast and smoothness that employ elastodynamic models and descriptions of their behaviour under the application of external and internal forces.

The objectives of this study were to develop an automatic method of Doppler velocity contour detection that could be implanted in standard echocardiographic systems, to eliminate the intra- and inter-observer variability. To validate this new method, data obtained with the new automatic detection method were compared to those obtained by the standard Doppler echocardiographic method.

## II. Methods

The active contour model (or snake) is an energy minimizing spline, whose energy depends on the snake's form and position in the image [6]. A snake is found after minimization of the energy functional, which is a sum of internal and external forces with weighting coefficients. A snake can be modeled as a parametric curve $v(s,t) = (x(s,t),y(s,t))$, where $x$ and $y$ are the coordinates of contour points, t is the current time or evolution step, and $s \in [0, 1]$ is the parametric domain and is proportional to the curve length. The energy functional that has to be minimized is defined as:

$$E_{snake} = \int_0^1 E_{in}\left[v(s,t)\right]ds + \int_0^1 E_{ex}\left[v(s,t)\right]ds \qquad (1)$$

In this equation,

- The internal snake's energy $E_{in}$ characterizes the deformation of a stretchy, flexible contour, and can be decomposed into a first and a second order term.

$$E_{in}\left[v(s,t)\right] = \frac{\alpha}{2}(s)\left|v_S(s,t)\right|^2 + \frac{\beta}{2}(s)\left|v_{SS}(s,t)\right|^2 \qquad (2)$$

E. Gaillard, Laboratory of Biomedical Engineering, Montreal Clinical Research Institute (IRCM), University of Montreal, Montreal, Canada (corresponding author's phone: 514-987-5722; fax: 514-987-5710; e-mail: emmanuel.gaillard@ircm.qc.ca)

L. Kadem, Laboratory for Cardiovascular Fluid Dynamics, Concordia University, Montreal, Canada (e-mail: kadem@encs.concordia.ca )

P. Pibarot, Quebec Heart Institute, Laval Hospital, Laval University, Sainte-Foy, Canada (e-mail: philippe.pibarot@med.ulaval.ca

L.-G. Durand, Laboratory of Biomedical Engineering, Montreal Clinical Research Institute (IRCM), University of Montreal, Montreal, Canada (e-mail: louis-gilles.durand@ircm.qc.ca

where $v_s(s,t) = \partial v(s,t)/\partial s$, $v_{ss}(s,t) = \partial^2 v(s,t)/\partial s^2$ and the coefficients $\alpha(s)$ and $\beta(s)$ control respectively the snake's tension and the snake's rigidity.

- The external snake's energy $E_{ex}$ acts on the snake determined from the image gradient. $\alpha$ and $\beta$ tend to shrink the curve while $E_{ex}$ tends to expand it.

$$E_{ex}\left[v(s,t)\right] = -P\left[v(s,t)\right] \tag{3}$$

where $P\left[v(s,t)\right]$ is a shape potential.

So the total energy of the snake (1) can be written as:

$$E_{snake} = \int_0^1 \frac{\alpha}{2}\left|v_s(s,t)\right|^2 + \frac{\beta}{2}\left|v_{ss}(s,t)\right|^2 - P\left[v(s,t)\right]\, ds \tag{4}$$

Original snakes did not solve contour detection problem completely. We needed to place the initial snake close to the real boundary of the object otherwise the snake did not converge to the correct result. Moreover, if a snake is initiated inside the object, the use of additional forces allowing the expansion the snake is required [13]. This limitation associated with the use of equation (4) can be overcome by using the generalized gradient vector flow field (GGVF) introduced by Xu and Prince [14] in 1998 instead of a potential field. Using GGVF, the snake does not need a prior knowledge about whether to shrink or expand toward the boundary and could be initialized far away from this one.

The initial positioning of the snake was determined from the automatic method developed by Tauber et al. [15] (Figures 1 and 2). This method is a generalization of the centers of divergence (CD) introduced by Xingfei and Tian [16]. These centers are the points where the GGVF vectors change one direction (weak divergence) or several directions (strong divergence) (Figures 1b and 2b).
Let $\mathrm{sign}(x)$ be a function showing the sign of $x$:

$$\mathrm{sign}(x) = \begin{cases} 1 & x > 0 \\ 0 & x = 0 \\ -1 & x < 0 \end{cases} \tag{5}$$

Then a set of CD for the vertical direction ($C_v$) and for the horizontal direction ($C_h$) of the vector field $v(i,j) = (a(i,j),\, b(i,j))$ can be defined as:

$$\begin{aligned} C_v &= \left\{ \begin{array}{l} (i,j) \mid a(i,j) \le a(i+1,j) \wedge \\ abs(\mathrm{sign}(a(i,j)) + \mathrm{sign}(a(i+1,j))) \le 1 \end{array} \right\} \\ C_h &= \left\{ \begin{array}{l} (i,j) \mid b(i,j) \le b(i,j+1) \wedge \\ abs(\mathrm{sign}(b(i,j)) + \mathrm{sign}(b(i,j+1))) \le 1 \end{array} \right\} \end{aligned} \tag{6}$$

Finally, the following definition for the set of the centers of weak divergence ($C_{weak}$) and for the set of the centers of strong divergence ($C_{strong}$) can be introduced:

$$\begin{aligned} C_{weak} &= \left\{ (i,j) \mid (i,j) \in C_v \vee (i,j) \in C_h \right\} \\ C_{strong} &= \left\{ (i,j) \mid (i,j) \in C_v \wedge (i,j) \in C_h \right\} \end{aligned} \tag{7}$$

The figures 1 and 2 show an example of CD calculated from two of our Doppler echocardiographic images. The centers of weak divergence (in blue on the figure) formed a kind of skeleton of the image, where the intersections are the centers of strong divergence (for the aortic flow, only one point occurs, whereas there are two points for the mitral flow due to the bi-wave (E and A waves) shape of the velocity profile). These centers of strong divergence were used as initial positions of the snake. For the aortic flow, the initial snake was a circle centered on the center of strong divergence, while for the mitral flow, the initial snake was an ellipse including the two centers of strong divergence and centered on the middle of the segment formed by these two centers. For the aortic flow, the initial size of the snake was determined from the length of the horizontal line including the center of strong divergence, demarcated by the edges of our velocity profile. These edges corresponded to the two points where the sign of the GGVF vectors changed from 1 to -1 (see equation 5). The circle diameter was fixed experimentally (that means that we have tested different initial sizes on several Doppler echocardiographic images) and corresponded to 1/3 of the length of this horizontal line (Figure 1c). For the mitral flow, the lengths of the major axis and the minor axis were also fixed experimentally and corresponded respectively to 1.3 times the "horizontal" distance between the two centers of strong divergence and 2.3 times the "vertical" distance between the two centers of strong divergence (Figure 2c).

Our active contour model was encoded under Matlab (The MathWorks, Inc.) and has been validated on simple geometries whose the shape was close to Doppler velocity echocardiographic images (triangles and trapezoids), with a maximal demarcated area difference below 2%.
Then, our new method was tested on Doppler echocardiographic images of left ventricular outflow tract and transvalvular flow velocity signals recorded in 30 patients, 15 with aortic stenosis and 15 with mitral stenosis. The tracing of the contour of the velocity envelope was performed manually by an experienced echocardiographer

## III. Results

The snake's evolution is represented on figure 3, for the aortic flow (top panel) and the mitral flow (bottom panel).
The results obtained with the automatic detection method were compared to those obtained manually. Comparison between the two methods has shown a very good agreement. The difference in terms of areas demarcated by the velocity contours was less than 7% for all measurements. To refine the comparison, we focused on three essential variables that are measured routinely by Doppler echocardiography in the clinical setting: the maximum velocity (Vmax), the mean velocity (Vmean) and the velocity-time integral (VTI) which

is one of the parameters allowing the determination of the valve effective orifice area (EOA), and then the severity of a stenotic valve. VTI is the area under the velocity-time curve. As shown in figure 4, there was a very good agreement between the two methods (mean correlation coefficient $R^2$ = 0.99 for each variable). To quantify the agreement between the two methods, Bland-Altman plots for the three variables were derived (Figure 4). Bias value between the two methods was small, about -2.7 cm/s (corresponding relative bias = 3.7%) for Vmax, about -4.4 cm/s (6.6%) for Vmean and about 0.66 cm (6%) for VTI, respectively. The limits of agreement were acceptable, -1.3% to 8.7% for Vmax, -1.9% to 15.2% for Vmean and -2.6% to 14.5% VTI, respectively.

## IV. Conclusions

We have validated our new automatic method of contour detection applied to Doppler velocity echocardiographic measurements of the mitral and aortic valve flow velocities. This detection method applied to Doppler velocity echocardiographic measurements could be useful to eliminate the intra- and inter-observer variability and measurements errors, and consequently to improve quantification of stenosis severity and ensuing clinical decision making. This automatic method could also allow the echocardiographer to realize these measurements within a much shorter period of time compared to standard manual tracing method. This new method could be easily implanted in standard echocardiographic system.

## References


[1] M. Galderisi, E. Benjamin, J. Evans, R. D'Agostino, D. Fuller, B. Lehman, et al., "Intra- and interobserver reproducibility of Doppler-assessed indexes of left ventricular function in a population-based study"., Am. J. Cardiol., vol. 70, pp. 1341-6, 1992.

[2] K. Bjornstad, M. al Amri, J. Lingamanaicker, I. Oqaili, L. Hatle, "Interobserver and intraobserver variation for analysis of left ventricular wall motion at baseline and during low- and high-dose dobutamine stress echocardiography in patients with high prevalence of wall motion abnormalities at rest", J. Am. Soc. Echocardiogr., vol. 9, pp. 320-8, 1996.

[3] F. Grothues, G. Smith, J. Moon, "Comparison of interstudy reproducibility of cardiovascular magnetic resonance with two-dimensional echocardiography in normal subjects and in patients with heart failure or left ventricular hypertrophy", Am. J. Cardiol., vol. 90, pp. 29-34, 2002.

[4] C. Kupfahl, M. Honold, G. Meinhardt, G. Vogelsberg, A. Wagner, H. Mahrholdt, et al., "Evaluation of aortic stenosis by cardiovascular magnetic resonance imaging: comparison with established routine clinical techniques", Heart, vol. 90, pp. 893-901, 2004.

[5] A.-D. Margulescu, M. Cinteza, D. Vinereanu, "Reproducibility in echocardiography: clinical significance, assessment, and comparison with other imaging methods", Maedica, vol. 1, pp. 29-34, 2006.

[6] M. Kass, A. Witkin, D. Terzopoulos, "Snakes: Active contour models" Int. J. Comput. Vis., vol. 1, pp. 321–31, 1988.

[7] T. McInerney and D. Terzopoulos, "Deformable models in medical image analysis: a survey". MIA, vol. 1, pp. 91–108, 1996.

[8] A. Singh, D. Terzopoulos, D. Goldgof, "Deformable Models in Medical Image Analysis", Los Alamitos: IEEE Computer Society Press, 1998.

[9] H. Sheshadri and A. Kandaswamy, "The role of active contour models in biomedical image analysis", AOIJ, pp. 14, 2005.

[10] D. Terzopoulos and R. Szeliski, "Tracking with Kalman snakes", In: Blake A., Yuille A. (Eds.). Active Vision. MIT Press, Cambridge, MA, pp. 3–20, 1992.

[11] A. Blake and M. Isard, "Active Contours", Springer-Verlag, Berlin, 1998

[12] H. Liu, G. Jiang, L. Wang, "Multiple objects tracking based on snake model and selective attention mechanism", IJIT, vol. 12, pp. 76-86, 2006.

[13] L. Cohen, "On active contour models and balloons", CVGIP: Image Understanding, vol. 53, pp. 211-8, 1991.

[14] C. Xu and J. Prince, "Generalized gradient vector flow external forces for active contours", Signal Processing, vol. 71, pp. 131–9, 1998.

[15] C. Tauber, H. Batatia, A. Ayache, "A robust active contour initialization and gradient vector flow for ultrasound image segmentation", Proceedings of Conference on Machine Vision Applications, Tsukuba Science City, Japan, pp. 164-7, 2005.

[16] G. Xingfei and J. Tian, "An automatic active contour model for multiple objects", Proceedings of 16th International Conference on Pattern Recognition, Quebec City, Canada, pp. 881-4, 2002.


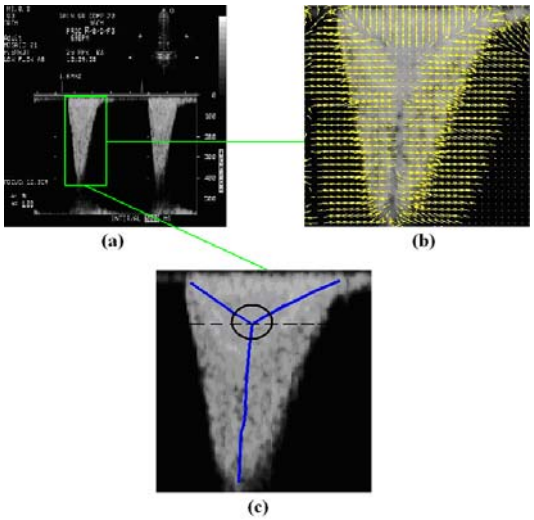


Fig. 1: Aortic flow. (a) Initial Doppler echocardiographic image. (b) Generalized gradient vector flow (GGVF) field (yellow vectors). (c) Centers of divergence (blue line), initial positioning and size of the snake (black circle) and the horizontal line allowing initializing the size of the snake (black dashed line).

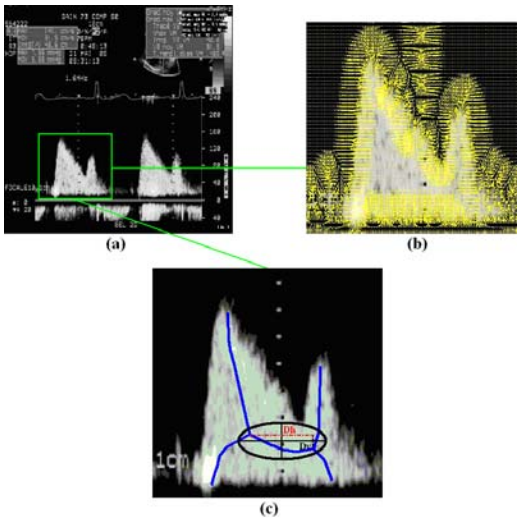


Fig. 2: Mitral flow. (a) Initial Doppler echocardiographic image. (b) Generalized gradient vector flow (GGVF) field (yellow vectors). (c) Centers of divergence (blue line), initial positioning and size of the snake (black ellipse), Dh and Dv mean respectively "horizontal" distance between the two centers of strong divergence and "vertical" distance between the two centers of strong divergence.

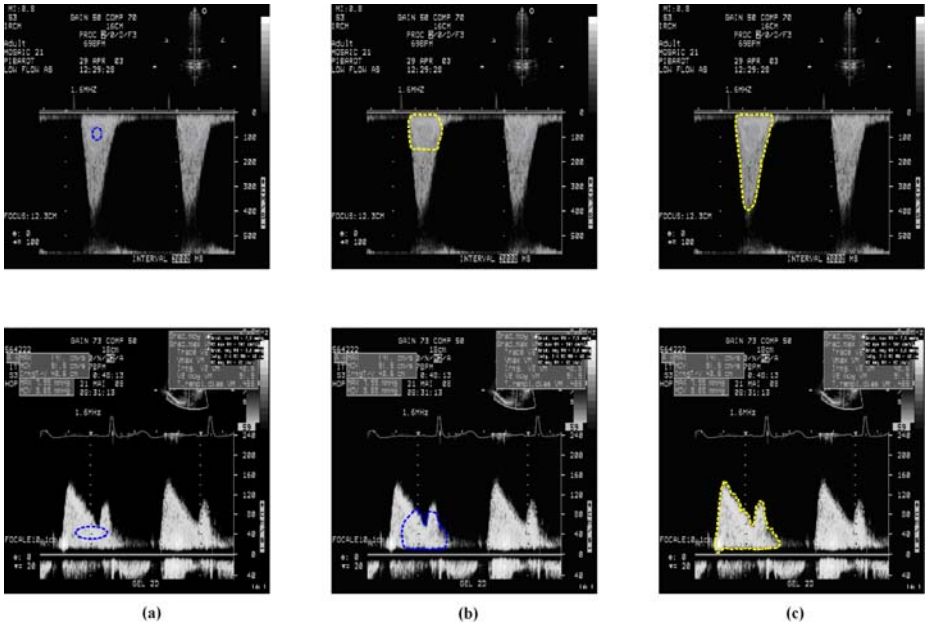


Fig. 3: Top panel: **aortic flow**; Bottom panel: **mitral flow**. (a) Initial positioning and size of the snake (blue dashed line). (b) Evolution of the snake (yellow dashed line for the aortic flow, blue dashed line for the mitral flow). (c) Final position of the snake (yellow dashed line).

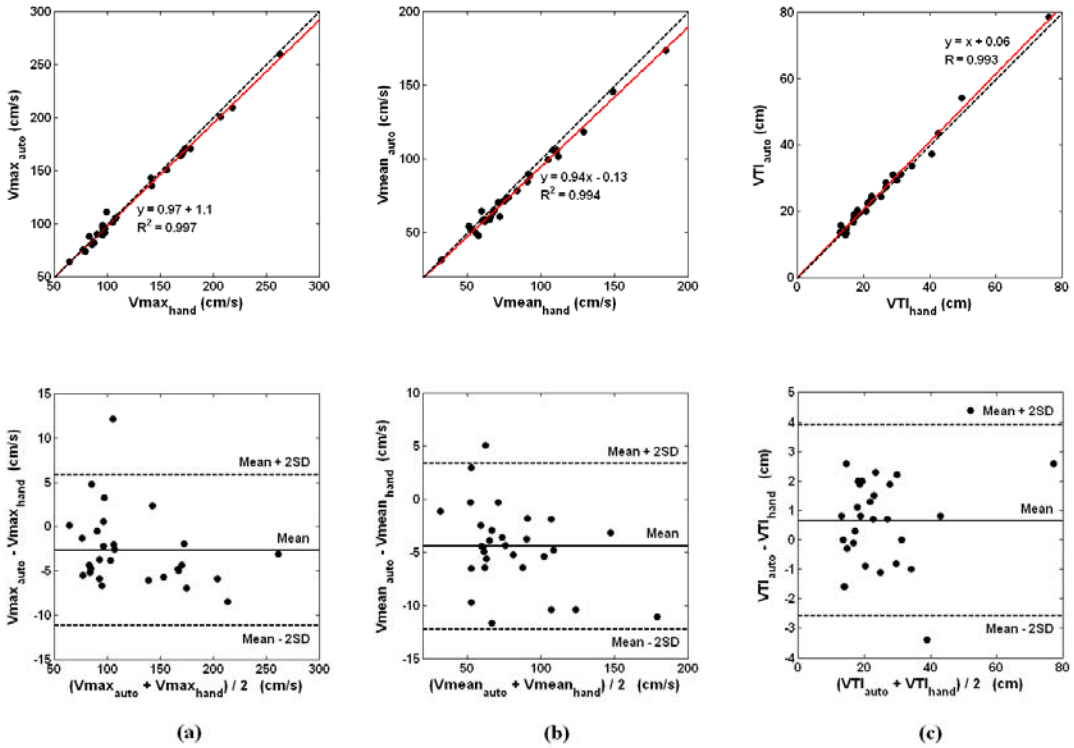


Fig. 4: Comparison between the automatic method and the manual tracing for three variables: (a) the maximum velocity (Vmax). (b) the mean velocity (Vmean). (c) the velocity time integral (VTI). $X_{auto}$ and $X_{hand}$ represent respectively the variable X obtained from the automatic method and obtained manually. At the bottom, Bland-Altman plots are represented.